*DOI:*
10.1021/acs.macromol.0c00409

*Document Version*
Peer reviewed version

# Threading different rings on X-shaped block-copolymers: hybrid pseudopolyrotaxanes of cyclodextrins and Tetronics

**Joan Puig-Rigall[1], Rafael Serra-Gómez[1], Nerea Guembe-Michel[1], Isabelle Grillo[2,†], Cécile A. Dreiss*[,3] and Gustavo González-Gaitano*[,1]**

[1] Departamento de Química, Universidad de Navarra, 31080 Pamplona, Spain
[2] Institut Laue-Langevin, 71 avenue des Martyrs, B.P. 156, 38042 Grenoble Cedex, France; grillo@ill.fr
[3] Institute of Pharmaceutical Science, King's College London, Franklin-Wilkins Building, 150 Stamford Street, London SE1 9NH, UK; cecile.dreiss@kcl.ac.uk
* Correspondence: gaitano@unav.es, cecile.dreiss@kcl.ac.uk

† As this manuscript was in preparation, our long-term colleague, ILL staff scientist, Isabelle Grillo passed away. We wish to dedicate this manuscript to her memory.

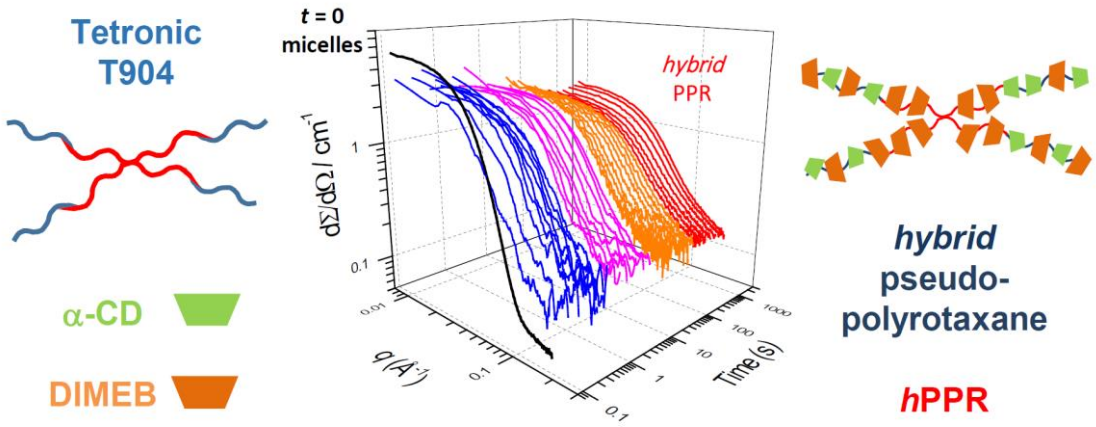

## Abstract

Pseudo-polyrotaxanes (PPRs) are supramolecular host–guest complexes constituted by the reversible threading of a macrocycle along a polymer chain. We report the formation of hybrid PPRs (hPPR), where two types of cyclodextrins thread either *simultaneously* or *sequentially* on 4-arm poly(ethylene-oxide)-poly(propylene-oxide) (PEO-PPO) block copolymers (Tetronic): native α-CD (with higher affinity for PEO) and dimethylated β-CD (DIMEB, with higher affinity for PPO). The competitive complexation along the chains is examined with three Tetronics, differing mainly in the length of their PEO blocks: T904, T1107 and T1307. While PPRs formed with α-CD are insoluble, due to the hydrogen-bond network formed between adjacent α-CD, the presence of DIMEB leads to soluble hybrid PPRs, slows down the kinetics of complexation, and increases the number of α-CD threaded per arm. The morphology of the species in solution over time was followed by time-resolved small-angle neutron scattering (TR-SANS) while their crystalline structure was studied by X-ray diffraction. While the complexation of the polymeric surfactant with DIMEB shifts the unimer-micelle equilibrium towards unimers, the presence of α-CD slows down demicellisation and reduces its extent. Overall, the co-threading of two cyclodextrins on the same polymer provides a handle to tune the complexation process and the final properties of the PPR, including solubility, kinetics of complexation, and composition of the complexes.



**Keywords:** cyclodextrins; Tetronic; block copolymers; micelles; polyrotaxanes; small angle neutron scattering (SANS); time resolved SANS

## 1. Introduction

Polyrotaxanes (PRs) are supramolecular mechanically interlocked structures in which macrocycles are threaded onto a polymer chain, forming a "molecular necklace",[1] where the ring-molecules are confined to the axle by stoppers at both ends of the polymer chain. In contrast, pseudopolyrotaxanes (PPRs) are not end-capped and the macrocycles are free to slide on and off the polymeric chain, according to the laws of chemical equilibrium and kinetics.[2,3] Most of the PRs and PPRs reported in the literature are produced with cyclodextrins (CDs), cyclic oligosaccharides of glucopyranose units arranged in a toroid shape.[4] The size of their apolar cavity, which depends on the number of glucopyranose molecules (6, 7, and 8 for the native α-, β-, and γ-CDs, respectively) determines the affinity for a specific polymer,[5] while the capacity to form hydrogen bonds between adjacent CDs contributes to stabilizing the resulting supramolecular structure.[6,7] The properties of native CDs, in particular solubility, can be tuned by substituting one, two or three of the hydroxyl groups on the glucopyranose unit, leading to "modified" CDs. The production, characterization and mechanisms of threading of CD-based PRs and PPRs have been extensively reviewed in the literature,[2,3,8] as well as the applications of these constructs as injectable hydrogels and scaffolds in tissue engineering.[9–12], sliding ring gels[13,14] and molecular machines.[15,16]

Since the pioneering work of Harada, it is known that water-soluble polymers based on EO or PO bind selectively to CDs:[1,17–19] α-CD forms insoluble PPRs with polyethylene oxide (PEO), but not with polypropylene oxide (PPO); instead, β- and γ-CD form PPRs with PPO but not with PEO.[6,7,17] This discrimination opens up interesting prospects with block-copolymers where each block shows selectively towards one type of CD. PPRs obtained with linear triblock-copolymers of PEO and PPO (poloxamers, or Pluronics) have been studied, with different block lengths of PEO and PPO, in combination with native[20,21] and

substituted CDs.[22–24] These constructs show promise, for instance for the treatment of Niemann-Pick Type C disease,[25–27] where 2-hydroxypropyl-β-cyclodextrin (HP-β-CD), delivered in the form of PRs, leads to improved pharmacokinetic profiles, bioavailability and larger reduction in the cholesterol pool, due to the longer circulating in blood of HP-β-CD threaded on a PR compared to CDs alone.[28] In comparison to Pluronics, there have been fewer studies on PPRs of poloxamines (or Tetronics),[29–33] a related family of block-copolymers where the PEO and PPO blocks are arranged in a cross-shape. Poloxamines display a rich phase behaviour, determined by block length and PEO:PPO ratio, a temperature-dependent micellisation and gelation,[34–38] as well as pH-responsiveness due to the central diamine group. These features, in addition to their inhibitory role on transmembrane efflux transporters, make them attractive candidates for targeted drug delivery.[39,40]

A limited number of studies to date have reported the co-threading of different cyclodextrins on the same chain, obtaining what we refer to as a "hybrid" PPR (hPPR).[28,41,42] The possibility of threading different rings on the same axle is attractive both from a fundamental perspective, to understand competitive binding processes where motion is restricted along one axis, and from a practical standpoint, as the combination of rotors can be used to optimize the properties of the supramolecular construct (e.g. solubility or toxicity profile[28]).

In this work, we report for the first time the formation of "hybrid" PPRs of Tetronic block-copolymers, T904, T1107 and T1307, having different HLBs and arm lengths (Table 1), with a combination of α-CD and DIMEB (a stereoregular methyl-substituted β-CD in positions 2 and 6). Specifically, we explore how the competitive binding of different CDs impacts the micellisation of the amphiphilic polymer, the solubility, stoichiometry and

crystalline structure of the precipitated PPRs formed, and how the order of addition of the macrocycles impacts the final structures of the PPRs.

## 2. Materials and Methods

*Materials*. Native cyclodextrins: α-cyclodextrin (≥98%, with water content of 10%, as determined by TGA) and modified cyclodextrins heptakis (2,6-di-O-methyl)-β-cyclodextrin (DIMEB, 1331 g·mol$^{-1}$, ≥98%) and randomly methylated β-cyclodextrin (DS ≈ 12) (RAMEB) (≥98%) were obtained from Sigma-Aldrich. Tetronic® 904 (T904), Tetronic® 1107 (T1107) and Tetronic® 1307 (T1307) were a gift from BASF (Table 1). All the solutions were prepared by weight, unless stated otherwise, and the concentrations are expressed in wt%.

**Table 1**. Structural properties of different poloxamines.

| **Tetronic** | $M_w$ **(g·mol$^{-1}$)** | $N_{EO}$ | $N_{PO}$ | **HLB** |
|---|---|---|---|---|
| T904 | 6700 | 15 | 17 | 12-18 |
| T1107 | 15000 | 60 | 20 | 18-23 |
| T1307 | 18000 | 72 | 23 | >24 |

$N_{EO}$, $N_{PO}$ are the number of monomers per PEO or PPO blocks, respectively.

*Gravimetric analysis.* Weighed amounts of the reactants were added to ensure final concentrations of 1% and 5% for Tetronic and α-CD, respectively, at different DIMEB concentrations (from 0% to 3%). Tetronic and CDs were mixed in 2.0 mL Eppendorf tubes. After 24 hours (long enough to guarantee that the solid PPR has completely formed) the dispersions were centrifuged for 10 minutes at 13000 rpm. The supernatant was removed, and the precipitate frozen at -80 ºC and lyophilized. The yield was obtained from the difference of mass with the empty tube as the mass of resulting solid divided by the total

mass of reactants. In the case of sequential additions of CDs, the second CD was added after 24 h.

*NMR spectroscopy.* Samples were prepared by re-dissolving a small amount of the dried precipitate obtained from gravimetric analysis in 500 μL DMSO-d6 (>99% purity) to fully dissociate the complex. 1D 1H-NMR spectra were recorded with a Bruker Advance 400 MHz spectrometer. To determine the stoichiometry of the complex, the number of CDs per Tetronic arm is calculated by measuring the areas of selected resonances from the polymer and the macrocycle, according to:

$$CDs/arm = \frac{A_{H1}/n}{A_{CH_3}/(3N_{PO})} \quad (1)$$

where $A_{H1}$ and $A_{CH3}$ are the areas of the signals from the outer H1 hydrogens of the CD and the methyl protons of the PO monomer of the Tetronic, respectively; *n* is the number of glucose units in the macrocycle (6 for α-CD and 7 for DIMEB); and $N_{PO}$ the number of PO monomers per arm (17 for T904, 20 for T1107 and 23 for T1307, Table 1). The experiments were run in duplicates.

*Turbidimetric analysis.* UV-visible spectra were recorded over time on an Agilent 8453 diode array spectrophotometer (2 nm resolution). Samples were placed in 1 cm path-length quartz cuvettes with magnetic stirring and temperature control incorporated (± 0.1 ºC, Quantum Northwest TC 1 accessory). The conditions set were 400 nm, a stirring speed of 1200 rpm, 40 ºC (to ensure the formation of micelles) and variable time intervals to produce a kinetic curve.

*X-ray diffraction (XRD).* Solid PPRs (samples from gravimetric analysis) were analysed at room temperature by X-ray powder diffraction (XRD) in a Bruker D8 Advance diffractometer. The Cu Kα1 radiation from the source was chosen, scanning from 5˚ to 40˚ (2θ), each 0.02˚ and 2 s per step.

*Time-Resolved SANS (TR-SANS).* Kinetic SANS experiments were carried out on the D22 diffractometer at the Institut Laue-Langevin (ILL), incorporating a stopped-flow unit (Biologic SFM-300), which allows for rapid mixing of solutions and triggers the reaction with data acquisition. The neutrons wavelength was set at 6 Å, the sample-to-detector distance at 4 m, with a collimation at 5.6 m and a detector offset of 400 mm, giving a wave vector range $1.2 \times 10^{-2} < q < 0.26$ Å$^{-1}$, with a $7 \times 10$ mm$^2$ sample aperture. The cell path length used was 1 mm and the temperature was set at 40ºC. The stock solutions of Tetronic and CD were prepared by weighing the required amounts of each compound and deuterated water. Appropriate volumes of stock solutions (total of 250 µL) were then mixed in the stopped-flow cell at a flow rate of 3 mL/s to obtain the target concentrations. Datasets of the experiments can be found on the ILL website.[43] SANS curves fitting was performed with SasView software in batch mode (data handling, fitting procedure and models used are described in Results and Discussion, SI and previous studies [44]).

## 3. Results and discussion

When mixing solutions of CDs and a suitable homopolymer, the macrocycles thread on the polymeric chain to form a PPR. If the polymer comprises different blocks, the CDs will interact selectively with different regions of the guest. In the case of poloxamines, the higher affinity of α-CD towards EO monomers leads to a preferential localization of the macrocycle on the outer PEO blocks, followed by precipitation of the PPR if the concentration of native CD is high enough.[33] Instead, DIMEB is expected to thread preferentially on the PPO blocks to produce a water-soluble PPR.[32] When both macrocycles are combined, the result is the formation of a "hybrid" PPR (hPPR). The order of addition of the CDs is expected to impact the structure and properties of the final construct; we

therefore examine the effect of simultaneous or consecutive addition on the kinetics of complexation and equilibrium structures.

*3.1 Simultaneous addition of α-CD and DIMEB: impact on PPR composition and solubility*

In the case of simultaneous addition, both CDs compete for the poloxamine, according to their different affinity for a specific block, with a random distribution expected along the four arms. The threading of the two CDs resulted in the precipitation of the PPR, implying the formation of hydrogen bonds between adjacent threaded CDs and the further bundling of the PPRs. The yields of the PPR formed for the different poloxamines are plotted in Figure 1, at fixed concentrations of α-CD (5%) and Tetronic (1%), and varying DIMEB concentration. Increasing the amount of DIMEB leads to a reduction of the mass of precipitate, the effect being more drastic for the shortest T904, for which no precipitate is obtained beyond 1% methylated CD.

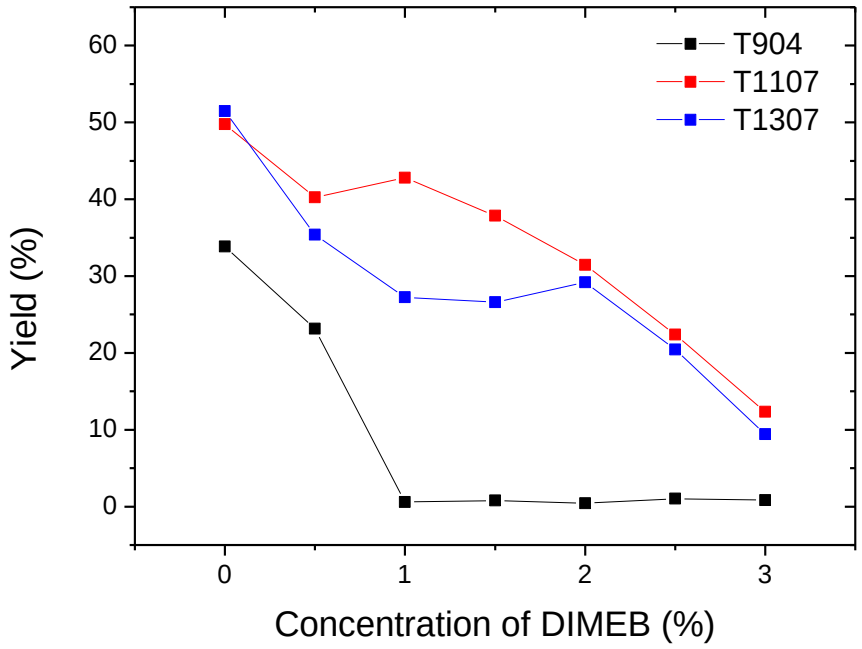


**Figure 1**. Yield of precipitated hybrid PPR as a function of DIMEB concentration (1% Tetronic and 5% α-CD) after simultaneous addition of both CDs.

The composition of the precipitated PPR, in terms of the number of α-CD and DIMEB included in the complex, can be obtained from NMR (Figure 2) by dissolving a small amount of the solid in DMSO and analysing the areas of selected resonances. In the absence of DIMEB, the number of α-CDs per arm varies with the poloxamine (6 for T904, 16 for T1107 and 18 for the longer T1307), in accordance with PEO block length (Table 2). The presence of DIMEB increases the number of α-CD threaded on the polymer (up to 18 and 22 α-CDs in T1107 and T1307, respectively, Figure 2A), a number close to the total concentration of α-CD initially present (Table 2), while the number of methylated CDs increases linearly with concentration (Figure 2B). Under these conditions (1% Tetronic and 5% α-CD), T904 was only studied at 0 and 0.5% DIMEB (where a precipitate is obtained), showing no change in composition of the PPR (data not shown).

**Table 2**. Number of α-CD molecules added, threaded and at saturation per arm of Tetronic, in the absence of DIMEB (1% poloxamine and 5% α-CD).

| **Tetronic** | **α-CD / arm $_{added}$*** | **α-CD / arm $_{threaded}$** | **α-CD / arm $_{saturated}$**** |
|---|---|---|---|
| T904 | 8.5 | 6 | 7.5 |
| T1107 | 19 | 16 | 30 |
| T1307 | 23 | 18 | 36 |

** Obtained from experimental concentrations (with 1% Tetronic and 5% α-CD) and molecular weights of the macrocycle (973 g·mol$^{-1}$) and poloxamines (Table 1).*
*** Theoretical values obtained for each Tetronic (Table 1), assuming that α-CD only complexes with the PEO block with a 2:1 EO:α-CD ratio.*

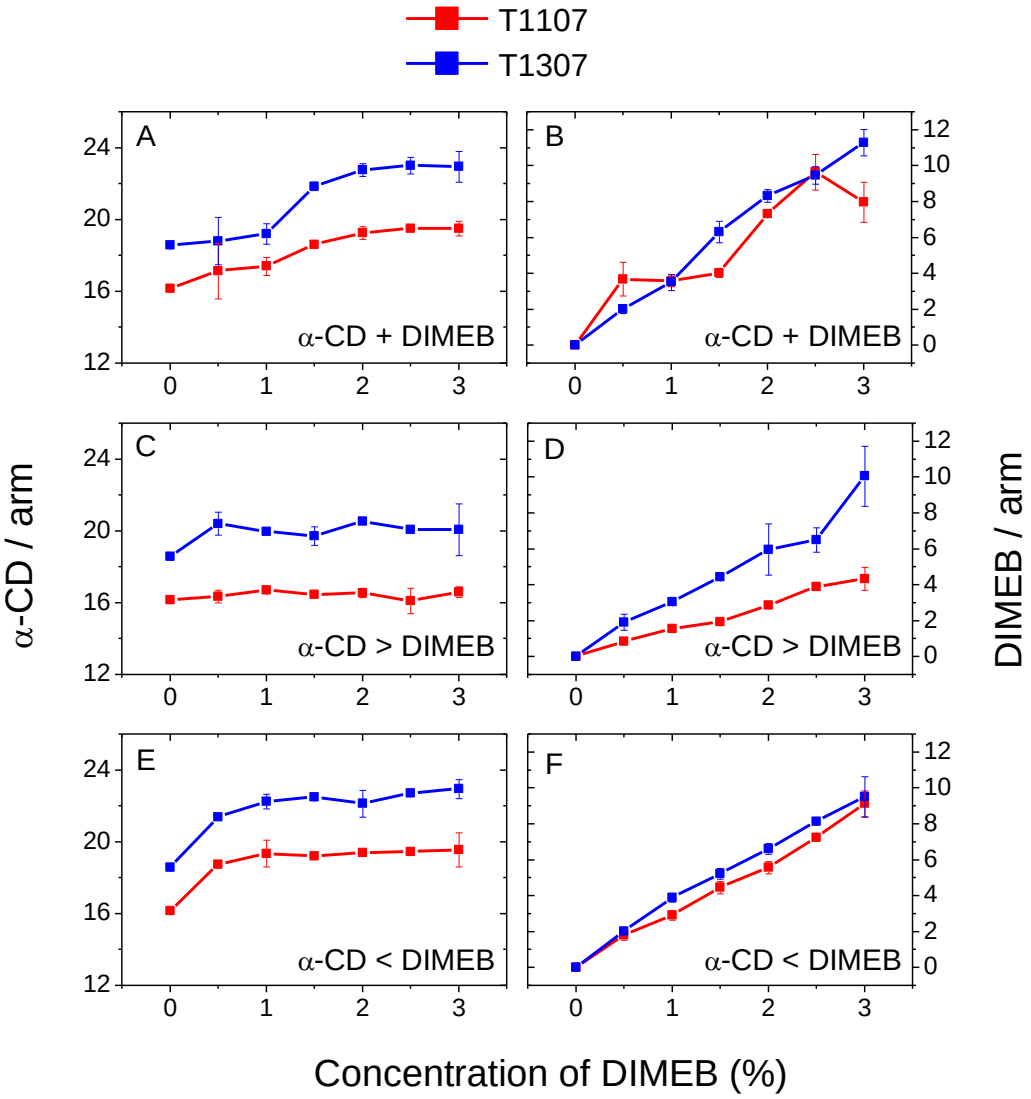


**Figure 2**. Number of α-CD and DIMEB per Tetronic arm as determined by NMR as a function of DIMEB concentration (1% Tetronic, 5% α-CD) after (A, B) simultaneous, (C, D) α-CD > DIMEB and (E, F) DIMEB > α-CD additions of both CDs.

Before its precipitation, soluble PPR must be present in the solution. The onset of turbidity (threading time, $t_{th}$) is an estimation of the average time to "cover" the polymer with enough CDs to induce precipitation, and can thus be used to monitor the kinetics of complexation.[45–48] In the absence of methylated CD, the precipitation is faster for shortest Tetronics ($t_{th}$ T1307 > T1107 > T904), at the same weight concentration (SI, Figure S1, Table 3, Figure 3).

**Table 3**. Threading times obtained from turbidimetry for the reaction at 40ºC of 1% Tetronic with 5% α-CD and DIMEB.

| | **Threading time ($t_{th}$ / min)** | |
|---|---|---|
| **% DIMEB** | **T904** | **T1307** |
| 0 | 15 | 90 |
| 0.5 | 25 | 100 |
| 1 | 240 | 120 |
| 3 | no precipitate | no precipitate |

Considering the previous results, as well as the fact that α-CD binds preferentially to EO (1 CD per two EO units), the four arms of T904 are expected to be almost covered by this macrocycle. With the longer T1107 and T1307, this is not the case (Tables 1 and 2), and there must be non-complexed domains of PEO, producing an uneven distribution of CDs that make the PPRs less likely to self-assemble further through hydrogen bonds, hence, it is more soluble. Saturation of the blocks corresponds to 30 and 36 α-CDs/arm for T1107 and T1307, respectively (Table 2), which is not reached in the conditions studied (SI, Figure S2). As the concentrations of DIMEB increases, precipitation is delayed, with no turbidity detected after 5 hours with any of the Tetronics at 3% DIMEB (Figure 3).

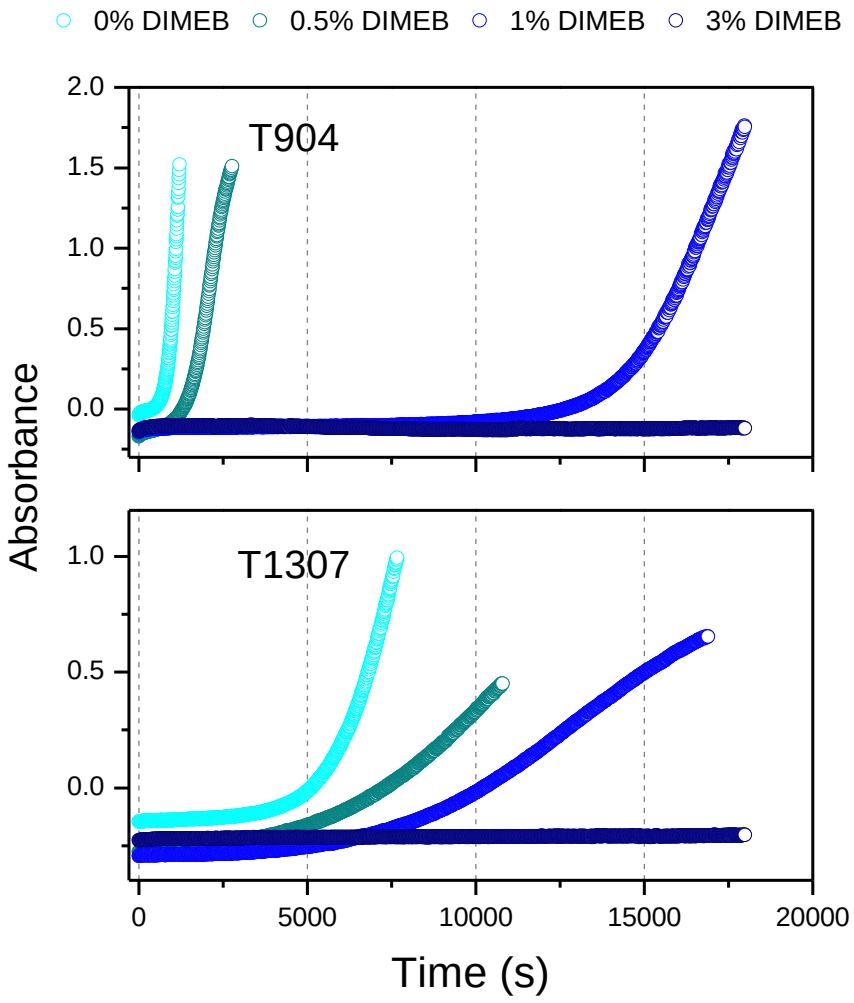


**Figure 3**. Kinetic profiles of PPR precipitation obtained from turbidimetry for the simultaneous addition at 40ºC of 5% α-CD and DIMEB (1% poloxamine).

The way the reaction has been carried out (simultaneous addition) implies a competition of both CDs, native and methylated, for the polymer, in which the threading takes place first through the external PEO blocks, for which α-CDs has more affinity. Therefore, the composition of the final PPR must reflect this different affinity, depending on copolymer length and concentration of CD. For example, at 1% and 3% of DIMEB, the ratio of α-CDs to DIMEB in the PPR for the two largest Tetronics varies from nearly 5:1 to 2:1, respectively, despite the amount of threaded α-CD increasing with DIMEB concentration (Figure 2A), thus reflecting the higher affinity of α-CD for the polymer. Overall, the different affinity of

the CDs is expected to induce, in all cases, random arrangements of the two CDs along the polymer, while the co-threading of DIMEB improves the complexation of α-CD and the solubility of the hybrid PPR.

*3.2 Threading at short times: kinetics of demicellisation*

At this point, it is interesting to investigate the PPR reaction at shorter times, when the PPR is forming but has not yet precipitated out of the solution. As these amphiphilic block copolymers self-assemble into micelles, the impact of the two cyclodextrins on the soluble PPRs can be assessed by studying the kinetics of demicellisation by time-resolved SANS (TR-SANS). It is necessary to work below the threshold of formation of the solid PPR, as it will give rise to high scattering and thus interfere with the data from the micelles. At 40ºC and 1% all the poloxamines considered in this work are well above their CMC.[32,49,50] The micellisation of the polymer is expected to compete with PPR formation, which, in turn, reduces the concentration of free unimers and consequently the number of micelles in solution.[33]

First, the effect of each CD (separately) on the micelles is shown in Figure 4 at different time points. The neutron scattering patterns for T1107 and T1307 upon addition of the native (α-CD, 2.5%) and modified CDs (DIMEB, 3% or RAMEB, 3%) reveal a loss in the scattering as the reaction proceeds for both poloxamines, showing the break-up of Tetronic micelles. With α-CD, the rupture of micelles is gradual, as evidenced by the loss of scattering over time, while it is much faster with DIMEB, with which a full rupture of the micelles is observed from the first timeframe (ca. 100 ms). Both the magnitude of this drop and the speed at which it takes place increases with increasing DIMEB concentration and it is particularly drastic at 3% DIMEB, irrespectively of the molar mass of the block copolymer (SI, Figure S3).

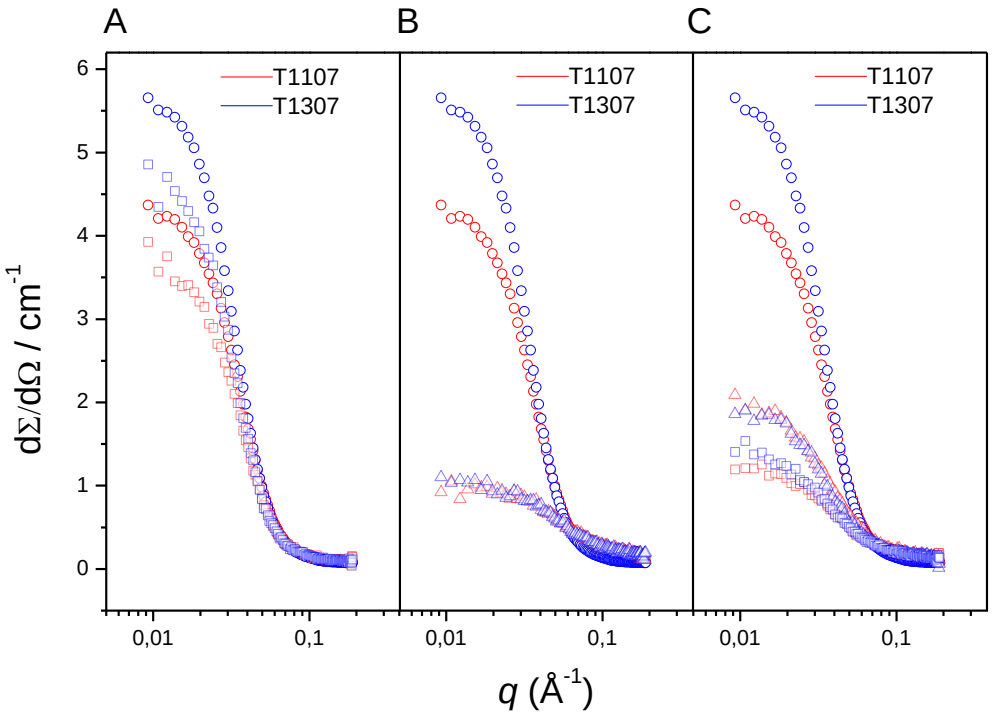


**Figure 4**. Time-resolved SANS patterns showing the disruption of T1107 and T1307 micelles with α-CD (A), DIMEB (B) or RAMEB (C) after 0 s (○) 10 s (△) and 3 min (□).

This effect of methylated CDs on shifting the unimer-micelle equilibrium has been reported for linear block copolymers[51,52] and other surfactants, like TPGS.[44] For example, using TR-SANS, it has been observed that Pluronic P85, P123 and F127 undergo fast micellar rupture with DIMEB, which has been ascribed to the existence of weak interactions between the PPO methyl groups and those of the primary and secondary rims of the macrocycle, leading to increased solubility.[53] Poloxamines differ from Pluronics with their 4-arm block structure but they are structurally similar, so the fast breakdown of the Tetronic micelles could also be attributed to these intermolecular methyl-methyl interactions, which do not exclude a simultaneous or further threading of the DIMEB on the hydrophobic central blocks. In fact, previous studies on T904 (by SANS and NMR) have shown that this poloxamine forms a soluble PPR with DIMEB, in which the CDs preferentially accumulate on the central PPO blocks, with a stoichiometry close to the expected 1CD per 2 PO units ratio,[21] and a certain degree of mobility along the arms.[32]

Based on this previous work, once the reaction begins, the solution is thus expected to contain micelles alongside a forming PPR, provided DIMEB concentration is low enough so as not to induce a total breakdown of the micelles. The overall neutron scattering thus comprises contributions from both structures, and a combined model that accounts for the scattering of each species has been used to analyse the SANS traces at each timeframe (4SP-CSS model, see SI for details). Some of the resulting parameters of the fits for T904 are shown in SI, Table S1. At low concentrations of DIMEB (0.5 and 1%), the decrease in micellar fraction is slow, and remains constant over long reaction times, similarly to the volume fraction and size of the resulting PPR.

At higher DIMEB concentration (3%), micelles are fully broken and only PPR is present in solution, so a simple 4-arm star model can be used to fit the PPR. The fitted quadratic radius of gyration is shown in SI, Figure S4, revealing a slight expansion in size of the growing PPR, from 23 Å (0.1 s) to 27 Å (1000 s), as the CDs are threading the polymer. Interestingly, replacing DIMEB by its randomly methylated counterpart, RAMEB, reduces the extent of micellar disruption and micelles are still present at the highest concentration (Figure 4C and SI, Table S1). This observation supports the hypothesis of methyl-methyl interactions being responsible for the breakdown of the micelles, but also a possible effect of the stereoregularity of the CD substitution on the matching of adjacent threaded CDs.

Having considered the kinetics with one CD, we finally turn to the kinetics obtained from the simultaneous addition of two different CDs, focusing on 1% T904 with 2.5% α-CD (below the threshold of PPR precipitation) and different DIMEB concentrations. The competition of both macrocycles to form the hybrid PPR is reflected in the scattering patterns. With 0.5 and 1% DIMEB, and using the same 4SP-CSS model, a small and progressive reduction of the micellar fraction is observed (Figure 5), similar to the absence of α-CD (SI, Table S1), albeit with a slightly higher fraction of micelles. At the highest

concentration of DIMEB (3%), a more sudden and drastic drop in micellar fraction is observed (Figure 5), however less extensive than the full demicellisation observed with DIMEB alone, where the full rupture of the micelles is observed from the first timeframe (SI, Figure S3).

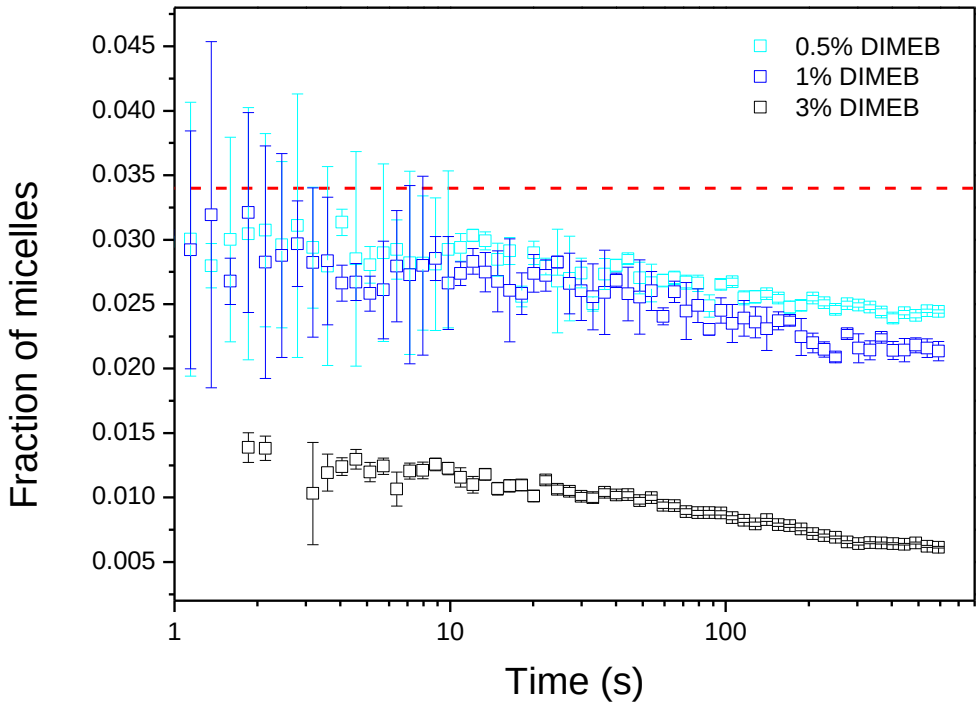


**Figure 5.** Data analysis from time-resolved SANS kinetics showing the evolution of the fraction of T904 micelles (1%), α-CD (2.5%) and different concentrations of DIMEB (0.5, 1, 3%) at 40 ºC after simultaneous addition of both CDs (red dash line is the micellar fraction at zero time, 0.034).

Overall, the study of the kinetics of complexation at short times and under conditions where precipitation does not take place, reveals a competitive process between PPR formation and de-micellisation. DIMEB induces a full and fast rupture of the micelles, a capacity that is reduced with RAMEB, and to a much reduced extent with α-CD, while the simultaneous addition of DIMEB and α-CD modulates micellar rupture.

*3.3 Consecutive addition of the CDs*

According to the different affinity of α-CD and DIMEB for the different blocks of the copolymer, the sequential addition of the macrocycles may affect the yields, the composition and the crystalline structure of the solid PPRs formed. For instance, if α-CD is added first, the PEO blocks should be complexed by this CD, subsequently hindering the further threading of DIMEB towards the central PPO blocks. The outcome, in terms of kinetics and final composition, should thus be different to the simultaneous addition, and consequently the yield or properties, such as solubility of the PPR, should differ.

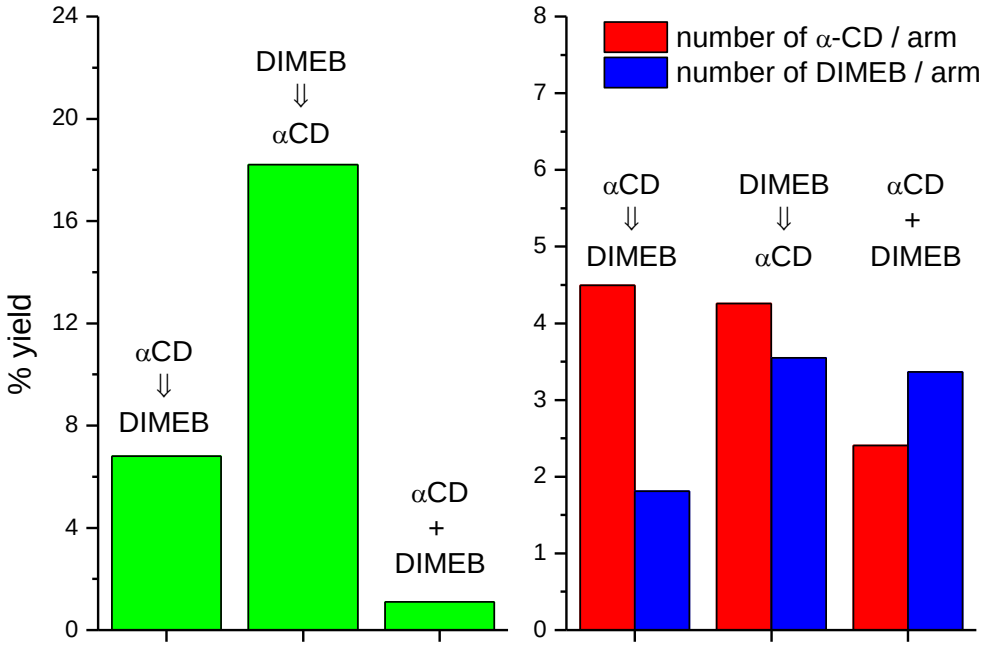


**Figure 6.** Comparison of PPR stoichiometry and yield for T904 (3%) under three different conditions of mixing: α-CD > DIMEB, DIMEB > α-CD, and simultaneous addition (3% α-CD, 6% DIMEB).

First, we consider the addition of α-CD before DIMEB (α-CD > DIMEB). In this case, the kinetic profiles (from turbidimetry) are the same as in the absence of DIMEB for each poloxamine and independent of the concentration of methylated CD, namely, DIMEB is not able to dissolve the solid PPR already formed with α-CD and its addition has no impact on the kinetic curves (data not shown). The yields decrease slightly with increasing amounts

of DIMEB for T1107 and T1307 (SI, Figure S5), and the same behaviour is observed for T904, with a yield that is higher at a high concentration of DIMEB (6 %) compared to the simultaneous addition (Figure 6, note the conditions studied are not the same as for T1107 and T1307). Regarding the number of macrocycles per arm for T1107 and T1307, the slight increase in the number of threaded α-CDs with increasing DIMEB concentration in the simultaneous addition (Figure 2A) is not observed here (Figure 2C). The number of DIMEBs per arm increase linearly, with about half the number of CDs threaded for the shorter T1107 (Figure 2D) compared to the simultaneous addition (Figure 2B). In the case of T904, the number of α-CDs is doubled, while DIMEB is halved compared to the simultaneous addition (Figure 6).

The fact that the number of threaded DIMEB increases upon increasing DIMEB concentration (for T1107 and T1307) suggests that some threading of DIMEB on the PEO blocks must take place. Thus, the addition in the order α-CD > DIMEB produces a hybrid PPR in which the PEOs would be covered mainly by α-CD, with some DIMEBs at the extremes of the external blocks. With T904, due to its small size, the PEO blocks are nearly saturated which explains the low number of additional CDs threaded (Figure 6).

We turn finally to the third reaction pathway, where DIMEB is added first, followed by α-CD (DIMEB > α-CD). For T1107 and T1307, precipitation occurs quickly with 0.5% DIMEB, it is delayed with 1% and no precipitation takes place with 3% DIMEB (SI, Figure S6 for T1107, data not shown for T1307), with yields similar to α-CD > DIMEB addition (SI, Figure S7). This way of conducting the reaction produces the highest yield of product for T904 (Figure 6). The number of α-CDs per arm is virtually constant with T1107 and T1307 (around 20 macrocycles, slightly higher compared to adding α-CD first, Figure 2E), while the number of DIMEBs increases with concentration, as in the simultaneous addition

(Figure 2F). The behaviour of T904 is similar to that of the larger surfactants. In this case, and comparing to other type of additions, the highest number of threaded α-CD (4-5 CDs per arm, as in the α-CD > DIMEB addition) and DIMEB (3-4 CDs per arm, as in the simultaneous one) is achieved with DIMEB > α-CD. Thus, independently of the type of Tetronic, the highest values of α-CD and DIMEB threaded on solid PPR are achieved with the sequence DIMEB > α-CD, because both CDs are accumulated on their preferential blocks (PPO for DIMEB and PEO for α-CD).

In conclusion, the sequential reaction pathway gives access to the selective accumulation of the cyclodextrins on their blocks of higher affinity, depending on the order of addition, giving rise to a block-like distribution of the macrocycles; instead, the simultaneous addition leads to a random arrangement of the macrocycles on the poloxamine arms, and a better solubility of the complexes. These different arrangements have direct consequences on the crystalline structure of the solid PPRs, as shown in the following section.

*3.4 Crystalline structure of hybrid PPRs*

Relevant information on the crystalline structure of the PPRs and the effect of the different reaction pathways can be obtained from XRD. The fingerprint of a solid PR formed from CDs is its diffraction pattern, characterized by two strong reflections at 19.9˚ and 22.7º, due to the channel-like arrangement of CDs threaded on the polymer chain, completely different to that of crystalline α-CD.[54] Diffractograms of the precipitates from the three poloxamines with α-CD show precisely these reflections (Figure 7), confirming the existence of channels of CDs in the solid PPR. Topchieva et al. have studied the XRD patterns of inclusion complexes (ICs) of PEG and α-CD on oriented samples, and assigned the most representative reflections.[55] According to this work, the peaks and the corresponding crystal planes (in brackets) that can be seen in Figure 7 correspond to 2θ = 7.5˚ (100), 13˚ (110),

19.9˚ (210) and 22.7˚ (300). In our case, the solid samples are not oriented as they have been produced by slow precipitation, but the peak positions must correspond to the same atom planes. Comparing the three PPRs, although the reflections are nearly the same, there are differences in the relative areas of the peaks at 20 and 23º, with values of 0.5, 2.4 and 3.6 for T904, T1107 and T1307, respectively (expressed as $A_{23}$ / $A_{20}$). As the number of PO units is comparable for the three Tetronic (Table 1), these differences have to be ascribed to the PEO blocks, on which α-CD threads preferentially. The lower intensities corresponding to the plane 210 (2θ = 19.9º) obtained for T1107 and T1307 point to a lower density of atoms in the *b* direction of the cell unit. As explained above, the four PEO blocks are nearly saturated by α-CD in T904 but the coverage is only partial with T1107 and T1307 (Table 2), which must therefore result in an uneven distribution of the macrocycles along the polymer arms.

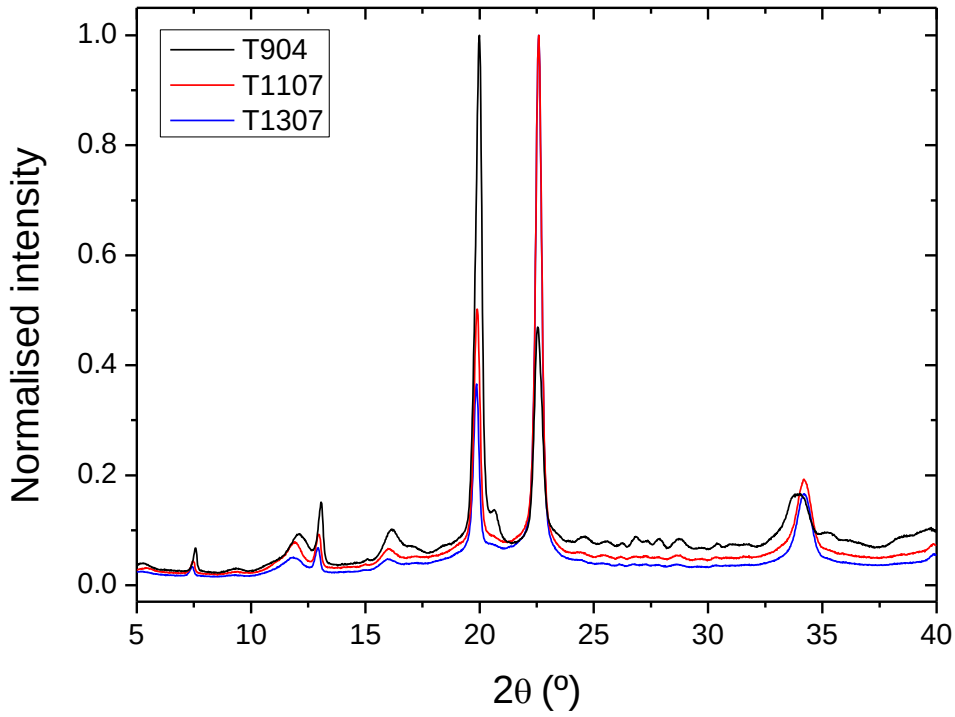


**Figure 7**. X-ray diffractograms from solid PPRs obtained with 1% Tetronic + 5% α-CD (T1107 and T1307 are completely overlapped at 2θ = 22.7˚).

The effect of introducing DIMEB and the order of addition (simultaneous or sequential, using 5% α-CD and 1% DIMEB) was studied with the shortest and longest poloxamines for comparison purposes. The simultaneous incorporation of both CDs to the PPR does not modify the diffraction patterns much (SI, Figure S8). For T904, a slight shift of the $2\theta$ = 19.9º peak to lower angles is observed in the presence of DIMEB, suggesting larger inter-planar spaces in the *b* direction, although $A_{23}$ / $A_{20}$ = 0.5 is obtained for both cases. The opposite behaviour is observed for T1307, in which no shift occurs, but the $A_{23}$ / $A_{20}$ ratio is doubled. Figure 8 shows the normalised traces for T1307 solid PPRs obtained from the sequential addition of the CDs. The channel-like stacking of α-CDs is present in both cases (intense reflections at $2\theta$ = 20º and 23º), but there are clear differences in the relative intensities. When the macrocycles are incorporated simultaneously, the regularity of the PPR is reduced, with the lowest value $A_{23}$ / $A_{20}$, corresponding to a structure that contains a random distribution of both CDs. Instead, the sequential addition produces blocks of grouped DIMEBs, preferentially localised towards the centre of the Tetronic (PPO blocks), and α-CDs on the outer PEOs (albeit less compact than in T904, given the length of the hydrophilic blocks in T1307, which did not lead to saturation at the concentrations used).

Thus, this more regular arrangement provides better packing features for the PPR chains. Adding α-CD first ($A_{23}$ / $A_{20}$ = 2.9) represents an intermediate situation between both, where DIMEB molecules, which enter after the PEO block is partially threaded by the native CD, may "push" the α-CDs further towards the centre, producing a somewhat more compact clustering of α-CDs, and a more efficient packing compared to that of α-CD alone with T1307 ($A_{23}$ / $A_{20}$ = 3.6). The most packed structures are obtained adding DIMEB first ($A_{23}$ / $A_{20}$ = 2.3), as it allows each CD to preferentially localise on the block with which they have a higher affinity. For both non-simultaneous additions, slightly more packed structures

are obtained at DIMEB concentration 3% compared to 1% (SI, Figure S9), with $A_{23}$ / $A_{20}$ ratios of 2.43 and 2.26, when adding first α-CD or DIMEB, respectively, in accordance with a higher number of threaded DIMEB (Figure 2).

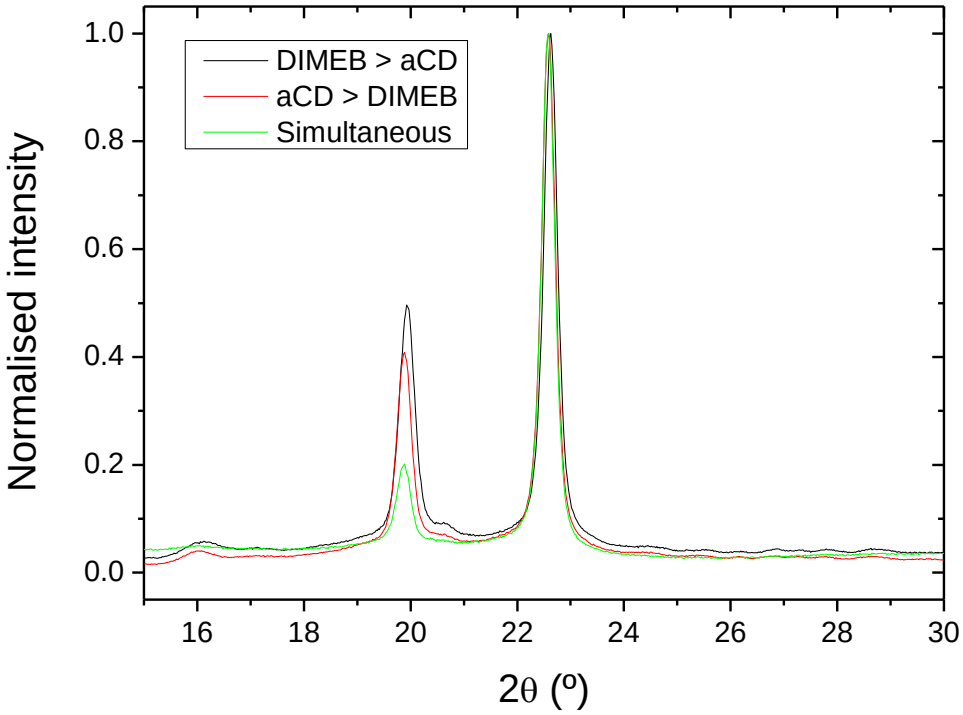


**Figure 8.** X-ray diffractograms from solid PPRs obtained with 1% T1307 + 5% α-CD + 1% DIMEB.

## 4. Conclusion

The formation of hybrid PPRs of Tetronic block-copolymers, T904, T1107 and T1307, having different arm lengths, with a combination of α-CD and DIMEB, has been investigated, with α-CD (smaller cavity) and DIMEB (larger cavity) forming inclusion complexes selectively with PEO and PPO, respectively. The objective was to examine how the competitive binding of the different CDs and their order of addition influences the kinetics of PPR formation and the composition of the final constructs.

The simultaneous addition of the two CDs leads to a competition of both macrocycles for the polymer to form a hybrid PPR, in which the CDs thread randomly. DIMEB hinders the formation of hydrogen bonds between neighbouring α-CD and on adjacent chains, preventing the PPR stacking and its further precipitation, and producing a more soluble construct with increasing amount of DIMEB, at an equivalent α-CD concentration. Above the CMT, the self-assembly of the Tetronic surfactants to form micelles is drastically modified by the presence of DIMEB, while the rupture of micelles with α-CD is partial and gradual with time, as shown by TR-SANS. Therefore, the break-down of the micelles can be modulated by the relative composition of both CDs in the reaction feed.

The sequential addition of macrocycles allows an organized arrangement of threaded CDs along the Tetronic unimers. Independently of which CD is added in first place and of the DIMEB concentration, higher yields of solid PPR are obtained. When α-CD is added first, the external PEO blocks are either partially or totally occupied with the native, narrower CD, limiting the entrance of DIMEB, and leading to an insoluble PPR, not too dissimilar to the case of α-CD alone. Instead, adding DIMEB first induces a preferential localisation of each CD on their preferred block, producing a "by-block" hybrid PPR with the most regular packing, as confirmed by XRD measurements, and with the highest number of both CDs threaded.

In summary, we have demonstrated the construction of hybrid PPRs from the co-threading of two different macrocycles, showing that the order of addition provides a handle to tune the properties of the supramolecular construct. In particular: the solubility of the PPR, kinetics of complexation, composition, complexation ratio, crystallinity of the solid PPR, while providing a new understanding into competitive binding processes restricted along one axis.

**Acknowledgments**

The authors acknowledge MINECO (Spain) for financial support through project MAT2014-59116-C2 and the Institut Laue-Langevin (ILL) for the provision of neutron beam time. J.P.-R. and R.S.-G. are grateful to the Asociación de Amigos de la Universidad de Navarra for their doctoral grant.

**Supporting information**

The supporting information is available free of charge on the ACS Publications website. TR-SANS curve analysis at various time points for T904 and methylated β-CDs at 40 ºC. Kinetic profiles for the reaction of α-CD with T904, T1107 and T1307 at 40 ºC. Composition of the solid PPR for α-CD with T1107 as a function of the CD concentration. TR-SANS showing the micellar disruption of T904 micelles at different concentrations of DIMEB. Evolution of the size of the soluble PPR formed during the reaction between DIMEB and T904. Yields for solid PPR formed after α-CD > DIMEB addition to T1107 and T1307 at various DIMEB concentrations. Kinetic profiles for T1107 with the sequential addition of DIMEB > α-CD. Yields of solid PPRs for T1107 and T1307 after DIMEB > α-CD addition at various DIMEB concentrations. X-ray diffractograms from solid PPRs obtained after simultaneous and non-simultaneous additions of CDs with T904 and T1307. Models used for TR-SANS data analysis with Sasview.

**References**

(1) Harada, A.; Li, J.; Kamachi, M. The Molecular Necklace: A Rotaxane Containing Many Threaded α-Cyclodextrins. *Nature* **1992**, *356* (6367), 325–327.

(2) Wenz, G. Cyclodextrins as Building Blocks for Supramolecular Structures and Functional Units. *Angew. Chemie Int. Ed. English* **1994**, *33* (8), 803–822.

(3) Nepogodiev, S. A.; Stoddart, J. F. Cyclodextrin-Based Catenanes and Rotaxanes. *Chem. Rev.* **1998**, *98* (5), 1959–1976.

(4) Szejtli, J. Introduction and General Overview of Cyclodextrin Chemistry. *Chem. Rev.* **1998**, *98* (5), 1743–1754.

(5) Davis, M. E.; Brewster, M. E. Cyclodextrin-Based Pharmaceutics: Past, Present and Future. *Nat. Rev. Drug Discov.* **2004**, *3* (12), 1023–1035.

(6) Harada, A. Preparation and Structures of Supramolecules between Cyclodextrins and Polymers. *Coord. Chem. Rev.* **1996**, *148*, 115–133.

(7) Pozuelo, J.; Mendicuti, F.; Mattice, W. L. Inclusion Complexes of Chain Molecules with Cycloamyloses. 2. Molecular Dynamics Simulations of Polyrotaxanes Formed by Poly(ethylene Glycol) and α-Cyclodextrins. *Macromolecules* **1997**, *30* (12), 3685–3690.

(8) Wenz, G.; Han, B. H.; Müller, A. Cyclodextrin Rotaxanes and Polyrotaxanes. *Chem. Rev.* **2006**, *106* (3), 782–817.

(9) Garcia-Rio, L.; Otero-Espinar, F. J.; Luzardo-Alvarez, A.; Blanco-Mendez, J. Cyclodextrin Based Rotaxanes, Polyrotaxanes and Polypseudorotaxanes and Their Biomedical Applications. *Curr. Top. Med. Chem.* **2014**, *14* (4), 478–493.

(10) Zhang, J.; Ma, P. X. Cyclodextrin-Based Supramolecular Systems for Drug Delivery: Recent Progress and Future Perspective. *Adv. Drug Deliv. Rev.* **2013**, *65* (9), 1215–1233.

(11) González-Gaitano, G.; Isasi, J. R.; Vélaz, I.; Zornoza, A. Drug Carrier Systems Based On Cyclodextrin Supramolecular Assemblies And Polymers: Present And Perspectives. *Curr. Pharm. Des.* **2017**, *23* (3), 411–432.

(12) Yu, G.; Yang, Z.; Fu, X.; Yung, B. C.; Yang, J.; Mao, Z.; Shao, L.; Hua, B.; Liu, Y.; Zhang, F.; et al. Polyrotaxane-Based Supramolecular Theranostics. *Nat. Commun.*

**2018**, *9* (1), 1–13.

(13) Liu, K. L.; Zhang, Z.; Li, J. Supramolecular Hydrogels Based on Cyclodextrin–polymer Polypseudorotaxanes: Materials Design and Hydrogel Properties. *Soft Matter* **2011**, *7* (24), 11290–11297.

(14) Okumura, Y.; Ito, K. The Polyrotaxane Gel: A Topological Gel by Figure-of-Eight Cross-Links. *Adv. Mater.* **2001**, *13* (7), 485–487.

(15) Ashton, P. R.; Grognuz, M.; Slawin, A. M. Z.; Stoddart, J. F.; Williams, D. J. The Template-Directed Synthesis of a [2]rotaxane. *Tetrahedron Lett.* **1991**, *32* (43), 6235–6238.

(16) Nobel Media AB. Sir J. Fraser Stoddart - Facts http://www.nobelprize.org/nobel_prizes/chemistry/laureates/2016/stoddart-facts.html (accessed Jun 5, 2018).

(17) Harada, A.; Kamachi, M. Complex Formation between Poly(ethylene Glycol) and α-Cyclodextrin. *Macromolecules* **1990**, *23* (10), 2821–2823.

(18) Harada, A.; Li, J.; Kamachi, M. Synthesis of a Tubular Polymer from Threaded Cyclodextrins. *Nature* **1993**, *364* (6437), 516–518.

(19) Tsai, C. C.; Leng, S.; Jeong, K. U.; Van Horn, R. M.; Wang, C. L.; Zhang, W. B.; Graham, M. J.; Huang, J.; Ho, R. M.; Chen, Y.; et al. Supramolecular Structure of β-Cyclodextrin and Poly(ethylene Oxide)-Block-Poly(propylene Oxide)-Block-Poly(ethylene Oxide) Inclusion Complexes. *Macromolecules* **2010**, *43* (22), 9454–9461.

(20) Harada, A.; Li, J.; Kamachi, M. Preparation and Properties of Inclusion Complexes of Polyethylene Glycol with Alpha-Cyclodextrin. *Macromolecules* **1993**, *26* (21), 5698–5703.

(21) Harada, A.; Okada, M.; Li, J.; Kamachi, M. Preparation and Characterization of

Inclusion Complexes of Poly(propylene Glycol) with Cyclodextrins. *Macromolecules* **1995**, *28* (24), 8406–8411.

(22) Gaitano, G. G.; Brown, W.; Tardajos, G. Inclusion Complexes between Cyclodextrins and Triblock Copolymers in Aqueous Solution: A Dynamic and Static Light-Scattering Study. *J. Phys. Chem. B* **1997**, *101* (5), 710–719.

(23) Dreiss, C. A.; Nwabunwanne, E.; Liu, R.; Brooks, N. J. Assembling and de-Assembling Micelles: Competitive Interactions of Cyclodextrins and Drugs with Pluronics. *Soft Matter* **2009**, *5* (9), 1888–1896.

(24) Bleta, R.; Machut, C.; Léger, B.; Monflier, É.; Ponchel, A. Coassembly of Block Copolymer and Randomly Methylated β-Cyclodextrin: From Swollen Micelles to Mesoporous Alumina with Tunable Pore Size. *Macromolecules* **2013**, *46* (14), 5672–5683.

(25) Mondjinou, Y. A.; McCauliff, L. A.; Kulkarni, A.; Paul, L.; Hyun, S.-H.; Zhang, Z.; Wu, Z.; Wirth, M.; Storch, J.; Thompson, D. H. Synthesis of 2-Hydroxypropyl-β-cyclodextrin/Pluronic-Based Polyrotaxanes via Heterogeneous Reaction as Potential Niemann-Pick Type C Therapeutics. *Biomacromolecules* **2013**, *14* (12), 4189–4197.

(26) Collins, C. J.; Loren, B. P.; Alam, M. S.; Mondjinou, Y.; Skulsky, J. L.; Chaplain, C. R.; Haldar, K.; Thompson, D. H. Pluronic Based β-Cyclodextrin Polyrotaxanes for Treatment of Niemann-Pick Type C Disease. *Sci. Rep.* **2017**, *7*, 1–13.

(27) Tamura, A.; Ohashi, M.; Yui, N. Oligo(ethylene Glycol)-Modified β-Cyclodextrin-Based Polyrotaxanes for Simultaneously Modulating Solubility and Cellular Internalization Efficiency. *J. Biomater. Sci. Polym. Ed.* **2017**, *28* (10–12), 1124–1139.

(28) Mondjinou, Y. A.; Loren, B. P.; Collins, C. J.; Hyun, S. H.; Demoret, A.; Skulsky, J.; Chaplain, C.; Badwaik, V.; Thompson, D. H. Gd3+:DOTA-Modified 2-Hydroxypropyl-β-Cyclodextrin/4-SulfobutylEther-β-Cyclodextrin-Based

Polyrotaxanes as Long Circulating High Relaxivity MRI Contrast Agents. *Bioconjug. Chem.* **2018**, *29* (11), 3550–3560.

(29) Larrañeta, E.; Isasi, J. R. Self-Assembled Supramolecular Gels of Reverse Poloxamers and Cyclodextrins. *Langmuir* **2012**, *28* (34), 12457–12462.

(30) Larrañeta, E.; Martínez-Ohárriz, C.; Vélaz, I.; Zornoza, A.; Machín, R.; Isasi, J. R. In Vitro Release from Reverse Poloxamine/α-Cyclodextrin Matrices: Modelling and Comparison of Dissolution Profiles. *J. Pharm. Sci.* **2014**, *103* (1), 197–206.

(31) Larrañeta, E.; Isasi, J. R. Non-Covalent Hydrogels of Cyclodextrins and Poloxamines for the Controlled Release of Proteins. *Carbohydr. Polym.* **2014**, *102*, 674–681.

(32) González-Gaitano, G.; Müller, C.; Radulescu, A.; Dreiss, C. A. Modulating the Self-Assembly of Amphiphilic X-Shaped Block Copolymers with Cyclodextrins: Structure and Mechanisms. *Langmuir* **2015**, *31* (14), 4096–4105.

(33) Puig-Rigall, J.; Serra-Gómez, R.; Stead, I.; Grillo, I.; Dreiss, C. A.; González-Gaitano, G. Pseudo-Polyrotaxanes of Cyclodextrins with Direct and Reverse X-Shaped Block Copolymers: A Kinetic and Structural Study. *Macromolecules* **2019**, *52* (4), 1458–1468.

(34) Alexandridis, P.; Athanassiou, V.; Fukuda, S.; Hatton, T. A. Surface Activity of Poly(ethylene Oxide)-Block-Poly(propylene Oxide)-Block-Poly(ethylene Oxide) Copolymers. *Langmuir* **1994**, *10* (8), 2604–2612.

(35) Alexandridis, P.; Holzwarth, J. F.; Hatton, T. A. Micellization of Poly(ethylene Oxide)-Poly(propylene Oxide)-Poly(ethylene Oxide) Triblock Copolymers in Aqueous Solutions: Thermodynamics of Copolymer Association. *Macromolecules* **1994**, *27* (9), 2414–2425.

(36) Nagarajan, R. Solubilization of Hydrocarbons and Resulting Aggregate Shape Transitions in Aqueous Solutions of Pluronic® (PEO–PPO–PEO) Block Copolymers.

*Colloids Surfaces B Biointerfaces* **1999**, *16* (1–4), 55–72.

(37) Kabanov, A. V.; Batrakova, E. V; Alakhov, V. Y. Pluronic® Block Copolymers as Novel Polymer Therapeutics for Drug and Gene Delivery. *J. Control. Release* **2002**, *82* (2–3), 189–212.

(38) Larrañeta, E.; Isasi, J. R. Phase Behavior of Reverse Poloxamers and Poloxamines in Water. *Langmuir* **2013**, *29* (4), 1045–1053.

(39) Cuestas, M. L.; Sosnik, A.; Mathet, V. L. Poloxamines Display a Multiple Inhibitory Activity of ATP-Binding Cassette (ABC) Transporters in Cancer Cell Lines. *Mol. Pharm.* **2011**, *8* (4), 1152–1164.

(40) Alvarez-Lorenzo, C.; Sosnik, A.; Concheiro, A. PEO-PPO Block Copolymers for Passive Micellar Targeting and Overcoming Multidrug Resistance in Cancer Therapy. *Curr. Drug Targets* **2011**, *12* (8), 1112–1130.

(41) Yang, C.; Ni, X.; Li, J. Synthesis of Polypseudorotaxanes and Polyrotaxanes with Multiple α- and γ-Cyclodextrins Co-Threaded over Poly[(ethylene Oxide)-Ran-(Propylene Oxide)]. *Polymer (Guildf).* **2009**, *50* (19), 4496–4504.

(42) Mondjinou, Y. A.; Hyun, S. H.; Xiong, M.; Collins, C. J.; Thong, P. L.; Thompson, D. H. Impact of Mixed β-Cyclodextrin Ratios on Pluronic Rotaxanation Efficiency and Product Solubility. *ACS Appl. Mater. Interfaces* **2015**, *7* (43), 23831–23836.

(43) Dreiss, C. A.; González-Gaitano, G.; Grillo, I.; Serra-Gómez, R. Unravelling the Mechanisms of Complexation between Tetronics and Cyclodextrins. *Inst. Laue-Langevin* **2015**, http://doi.ill.fr/10.5291/ILL-DATA.9-12-401.

(44) Puig-Rigall, J.; Grillo, I.; Dreiss, C. A.; González-Gaitano, G. Structural and Spectroscopic Characterization of TPGS Micelles: Disruptive Role of Cyclodextrins and Kinetic Pathways. *Langmuir* **2017**, *33* (19), 4737–4747.

(45) Lo Nostro, P.; Lopes, J. R.; Cardelli, C. Formation of Cyclodextrin-Based

Polypseudorotaxanes: Solvent Effect and Kinetic Study. *Langmuir* **2001**, *17* (15), 4610–4615.

(46) Lo Nostro, P.; Giustini, L.; Fratini, E.; Ninham, B. W.; Ridi, F.; Baglioni, P. Threading, Growth, and Aggregation of Pseudopolyrotaxanes. *J. Phys. Chem. B* **2008**, *112* (4), 1071–1081.

(47) Serres-Gómez, M.; González-Gaitano, G.; Kaldybekov, D. B.; Mansfield, E. D. H.; Khutoryanskiy, V. V.; Isasi, J. R.; Dreiss, C. A. Supramolecular Hybrid Structures and Gels from Host–Guest Interactions between α-Cyclodextrin and PEGylated Organosilica Nanoparticles. *Langmuir* **2018**, *34* (36), 10591–10602.

(48) Ceccato, M.; Lo Nostro, P.; Baglioni, P. α-Cyclodextrin/Polyethylene Glycol Polyrotaxane: A Study of the Threading Process. *Langmuir* **1997**, *13* (9), 2436–2439.

(49) Serra-Gómez, R.; Dreiss, C. A.; González-Benito, J.; González-Gaitano, G. Structure and Rheology of Poloxamine T1107 and Its Nanocomposite Hydrogels with Cyclodextrin-Modified Barium Titanate Nanoparticles. *Langmuir* **2016**, *32* (25), 6398–6408.

(50) González-Gaitano, G.; da Silva, M. A.; Radulescu, A.; Dreiss, C. A. Selective Tuning of the Self-Assembly and Gelation of a Hydrophilic Poloxamine by Cyclodextrins. *Langmuir* **2015**, *31* (20), 5645–5655.

(51) Valero, M.; Dreiss, C. A. Growth, Shrinking, and Breaking of Pluronic Micelles in the Presence of Drugs And/or β-Cyclodextrin, a Study by Small-Angle Neutron Scattering and Fluorescence Spectroscopy. *Langmuir* **2010**, *26* (13), 10561–10571.

(52) Valero, M.; Grillo, I.; Dreiss, C. A. Rupture of Pluronic Micelles by Di-Methylated β-Cyclodextrin Is Not Due to Polypseudorotaxane Formation. *J. Phys. Chem. B* **2012**, *116* (4), 1273–1281.

(53) Castiglione, F.; Valero, M.; Dreiss, C. A.; Mele, A. Selective Interaction of 2,6-Di-

O-Methyl-β-Cyclodextrin and Pluronic F127 Micelles Leading to Micellar Rupture: A Nuclear Magnetic Resonance Study. *J. Phys. Chem. B* **2011**, *115* (29), 9005–9013.

(54) Sabadini, E.; Cosgrove, T.; Taweepreda, W. Complexation between α-Cyclodextrin and Poly(ethylene Oxide) Physically Adsorbed on the Surface of Colloidal Silica. *Langmuir* **2003**, *19* (11), 4812–4816.

(55) Topchieva, I. N.; Tonelli, A. E.; Panova, I. G.; Matuchina, E. V.; Kalashnikov, F. A.; Gerasimov, V. I.; Rusa, C. C.; Rusa, M.; Hunt, M. A. Two-Phase Channel Structures Based on α-Cyclodextrin−Polyethylene Glycol Inclusion Complexes. *Langmuir* **2004**, *20* (21), 9036–9043.